Postprint of: Zima B., Wołoszyk K., Garbatov Y., Experimental and numerical identification of corrosion degradation of ageing structural components, OCEAN ENGINEERING, Vol. 258 (2022), 111739, DOI: 10.1016/j.oceaneng.2022.111739

Experimental and numerical identification of corrosion degradation of ageing structural components

Beata Zima[a], Krzysztof Woloszyk[a], Yordan Garbatov[b, 1]

[a] *Institute of Ocean Engineering and Ship Technology, Gdansk University of Technology, G. Narutowicza 11/12 st., 80-233 Gdansk, Poland*
[b] *Centre for Marine Technology and Ocean Engineering (CENTEC), Instituto Superior Técnico, Universidade de Lisboa, Avenida Rovisco Pais 1049-001 Lisboa, Portugal*

Abstract

The study presents experimental and numerical identification of corrosion degradation of thin-walled structural components employing guided wave propagation. The steel structural components are subjected to through-thickness varying corrosion degradation levels. The developed approach using the non-destructive guided wave-propagation quantifies the equivalent average corrosion degradation level exploring a limited number of transducers. A group velocity dispersion curve reconstruction has been used to determine the corrosion-induced plate thickness reduction. Two case studies are used to examine experimentally the newly developed approach. In the first one, the dispersion curve and the assessment of the corrosion thickness reduction have been made using wave signals of various excitation frequencies. In the second one, the analysis has been conducted only for two wave propagation signals and one excitation frequency which allowed for reconstructing the dispersion curve in a limited frequency range. In both case studies, a good agreement between the natural and estimated corrosion degradation levels was observed. The present study develops a signal processing methodology, which can be used in the SHM systems, where several aspects still need to be further investigated before it can be applied in large size and complex geometry of ship hull structures.

Keywords:

corrosion degradation; steel plates; ship structures; NDT; ultrasonic waves

1 Introduction

Ships and offshore structures are operating in a highly corrosive environment. The excessive corrosion degradation may lead to catastrophic consequences, e.g., exceedance of the

[1] Corresponding author e-mail: yordan.garbatov@tecnico.ulisboa.pt; Telf (351) 21 841 7907

ultimate strength of ship structural components (Woloszyk et al., 2018) and entire ship hull (Parunov et al., 2007). According to Zayed et al. (Zayed et al., 2018), even up to 90% of ship hull damages are primarily or indirectly caused by corrosion. An example of tanker ship loss, mainly driven by excessive corrosion degradation, breaking the ship's hull in two parts, is the tanker Prestige in 2002 (Flashback history: Tanker Prestige sinking (Video), 2015).

There are regular surveys of the entire ship to avoid severe degradation, where the thickness of structural components is measured using an ultrasonic thickness gauge. This method has various advantages, i.e., the equipment is portable, and the usage is user-friendly. However, it provides information about thickness in one point of any particular measurement. Thus, numerous thickness measurements must be done to correctly map the distribution of thickness corrosion diminutions within larger structures like ship hulls.

Cegla and Gajdacsi (Cegla and Gajdacsi, 2016) found that irregularities in corroded surfaces disturb the ultrasonic measurements and usually overestimate the corroded plate thickness value. Similar observations have been found in (Woloszyk et al., 2021). Zayed et al. (Zayed et al., 2008) analysed the factors that may disturb the ultrasonic measurements, e.g. lighting, cleanliness and accessibility to the inspected area. Additionally, there is always a probability that some deteriorated structural components are omitted during the inspections. Such a possibility may be seen in a more difficult area for inspection as double bottom or closed spaces.

To reflect some problems faced with using the non-destructive measuring techniques, some new approaches were developed, especially based on guided waves, which were proved to be very useful in diagnostics of both localized damages (Cao et al., 2021; Wandowski et al., 2011; Zima, 2021), as well as surface damages (Ding et al., 2021; Hu et al., 2022; Zima and Rucka, 2017). The guided wave propagation seems to define the corrosion degradation level around the structural components effectively. The most advantageous feature of the guided wave propagation approach is mapping a larger area of the thickness of structural components. Moreover, high-frequency wave-based methods are generally insensitive to applied loads and low-stress levels (the differences in wave velocities are negligible), which significantly facilities the analysis and results interpretation (Li et al., 2021).

Ervin and Reis (Ervin and Reis, 2008) tested the guided waves' low and high-frequency ranges to monitor the reinforced bar's corrosion degradation in mortar specimens. Ervin et al. (Ervin et al., 2009) used longitudinal ultrasonic waves of high frequencies to monitor the reinforced mortar specimens undergoing accelerated uniform and localised corrosion.

Two ultrasonic techniques of pulse transmission and pulse-echo were used to monitor the healthy and damaged bar by Sharma and Mukherje (Sharma and Mukherjee, 2010). Fractal analysis of guided ultrasonic waves for evaluating the corrosion degradation level in post-tensioned systems was proposed by Moustafa et al. (Moustafa et al., 2014). Farhidzadeh and Salamone (Farhidzadeh and Salamone, 2015) used dispersion curves, continuous wavelet transform, and wave velocity measurement to quantify the corrosion damage of multiwire prestressing steel strands.

In all reported cases, the corrosion degradation was accelerated by applying the direct current. The level of corrosion degradation (mass loss) was linearly dependent on corrosion current and time elapsed. The corrosion degradation assessment was based on the analysis of the dispersion curves. Because the shape of dispersion curves mainly depends on the geometric parameters, monitoring the trace changes efficiently assessed the corrosion degradation level.

Recently the methods of dispersion curve reconstruction have been extensively studied. However, the dispersion curve reconstruction demands multiple measurements along the relatively short propagation path, which would be inefficient in a large-scale structure like offshore platforms or ships (Draudviliene et al., 2021). Finally, there are almost no studies regarding guided wave propagation to identify the corrosion degradation of thin-walled structures subjected to environmental corrosion. Most of the studies were related to localised pitting corrosion (Ciampa et al., 2015; Ding et al., 2021; Howard and Cegla, 2017; Hua et al., 2020; Tian et al., 2021). The corrosion degradation observed in ship structures is mainly general (Panayotova and Garbatov, 2010), although pitting one is quite common too. General corrosion is observed, e.g., in cargo holds as well as in ballast tanks.

Recently, the study aimed at a corrosion assessment using the guided ultrasonic waves (Zima et al., 2022), contained a detailed description of a methodology based on the phase velocity and convex optimization. The study performed here is the next step aimed at procedure simplification and reducing the extent of the sensors network, as well as the collected data in the future SHM systems. Previously employed phase velocity was determined using spectral decomposition and the zero-cross method. Because of the dispersive nature of guided waves and spreading the wave packet, the unambiguous identification of corresponding roots may be associated with impediments to interpretation. Moreover, it was proved that usually the phase velocity is overestimated which leads to underestimation of corrosion degradation level [20]. Therefore, in the following study, the approach based on dispersion curve reconstruction has been modified and we have used the Hilbert transform and group velocity curve to assess the degradation level of thin-walled ship structures. Such modifications allow for simplification of

the signal processing procedure. The newly developed approach's main advantage is that only two adjacent wave propagation signals are needed in the identification process. The limited number of essential signals processed within the algorithm is extremely important from the point of view of the further development of the diagnostics systems and data communication. The smaller number of signals requires fewer measurements which in turn means a smaller size of memory and the whole size of the potential devices. Additionally, the smaller size of the device and a limited number of excitations and registrations entail longer battery life and lower costs of equipment maintenance. Although the presented algorithm is only the first step in the development of the diagnostics methods for ship structural monitoring and its requirement improvements which are faithfully discussed in the paper, the small amount of necessary data is one of its most significant advantages.

The corrosion degradation level of a significant area may be assessed, which makes the newly developed approach far more effective than the standard one of the ultrasonic thickness measurement or wave tomography. The analysed corroded thin-walled structural components were initially corroded employing an originally designed corrosion deterioration set-up. The corrosion degradation process was in line with in-situ environmental degradation. The designed corrosion deterioration set-up has a significant advantage over the efficient DC-induced corrosion degradation and leads to more realistic surface characteristics (Xiao et al., 2020; Yuan et al., 2007), but is still very different from the real one.

Based on the obtained reconstructed dispersion curves the corrosion degradation level has been assessed. To analyse the effectiveness and accuracy of state assessment of the specimen, the analysis stage has been divided into two stages. Within the first stage, five different frequencies were used in the study and the curves have been reconstructed in the wide frequency range. At the second stage, the curve was traced only for a narrow frequency range reconstructed after one excitation. In both cases, the progress of corrosion degradation affected the shape of the curves. The results collected within both stages were compared with the actual one determined by mass calculation. The agreement between the results suggests the potential of the novel method in corrosion degradation monitoring. The article discusses both advantages and disadvantages of the proposed method.

2 Guided waves propagation in thin-walled structures

2.1 Theoretical background

The guided waves in plates are generated due to the interaction of compressive and shear waves propagating in elastic, homogeneous, isotropic medium bounded with two equidistant surfaces. Horace Lamb foresaw their existence (Lamb, 1917) and derived dispersion equations relating to the propagation velocity and the number of possible wave modes with an excitation frequency. In general, the Lamb waves can exist as symmetric and antisymmetric. They are high dispersive, and their propagation velocity depends on the frequency and plate thickness product. Two equations describe the dispersive characteristics of both types:

$$\frac{\tan(qd)}{\tan(pd)} = -\frac{\left(k^2 - q^2\right)^2}{4k^2 pq}, \tag{1a}$$

$$\frac{\tan(qd)}{\tan(pd)} = -\frac{4k^2 pq}{\left(k^2 - q^2\right)^2} \tag{1b}$$

where d is the plate thickness and the parameters p and q depend on wavenumber k, angular frequency ω, longitudinal wave velocity (c_L) or shear wave velocity (c_T) in the infinite medium. The velocities of guided and bulk waves depend also on the material parameters of the considered medium. Eqn 1a is associated with symmetric particle motion about the midplane, while Eqn 1b describes the antisymmetric particle motion caused by wave propagation. The number of possible solutions fulfilling the Eqn (1) is infinite, and in general, the roots may be complex. However, the real roots are associated with propagating waves, while imaginary roots corresponding to evanescent waves will not be considered in further analysis. The solution of the dispersion equation is presented in the form of dispersion curves. At least one symmetric mode (S) resembling axial waves and one antisymmetric mode (A) resembling flexural wave exists for each frequency. The number of possible curves associated with any particular wave mode increases with the increase of the considered frequency range. The exemplary dispersion curves traced for a steel plate are presented in Figure 1.

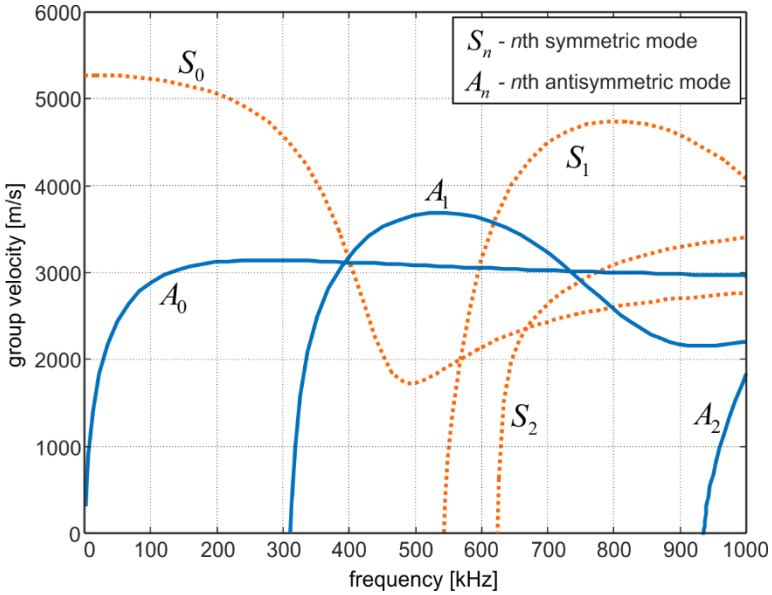

Figure 1 Dispersion curves for a steel plate with a thickness of 5 mm, elastic modulus E = 198 GPa, ν = 0.3 and density 7,850 kg/m^3

It has to be pointed out that the Lamb theory is valid only for plates with constant thickness, and their material fulfils the conditions of elasticity, homogeneity, and isotropy. Meanwhile, the corroded specimens are usually covered with corrosion products varying in mechanical properties from the undamaged core. In general, the additional layers require different wave theories, but in the following study, the corrosion products were removed before the investigation to assess the damage degradation level. This research will verify the correctness of the assumption about the constant thickness.

2.2 Signal processing procedure

As mentioned, the shape of dispersion curves depends on the material and geometric parameters of the considered plate. The proposed approach for a corrosion level assessment assumes that corrosion degradation influences the thickness of the plate. At the same time, the elastic modulus, density, and Poisson's ratio are considered to remain unaffected. In consequence, the shape of the dispersion curve depends on the corrosion deterioration level. In general, the assumption about the constant material parameters is not valid for cases of corroded structures and will be verified in this study. However, the plate thickness is the most influential factor, and its variation affects the wave velocity the most. Figure 2 presents the dispersion curve associated with the first antisymmetric Lamb mode in the frequency range (0-500 kHz) for steel plates with varying thicknesses. For some frequencies, the degree in the group propagation velocities is significant (i.e., 100 kHz). In contrast, for some frequencies, the curves

coincide with each other, which indicates that the corrosion degradation (plate thickness reduction) does not impact the wave propagation (i.e., 400-500 kHz).

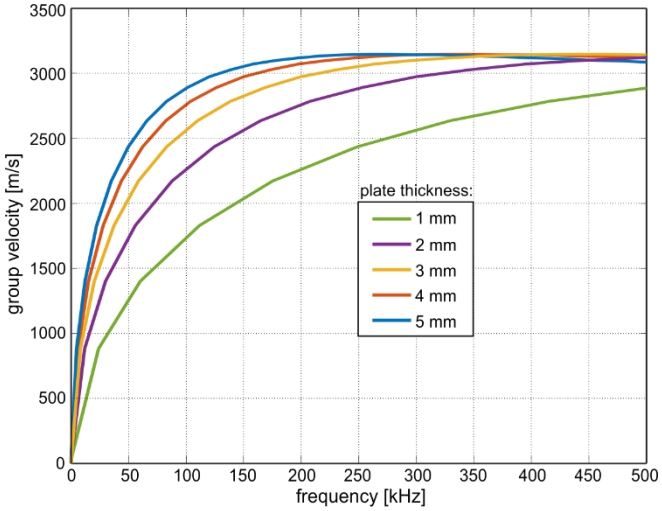

Figure 2 Dispersion curve associated with the first antisymmetric Lamb mode for plates with a varying thickness

Moreover, the corrosion degradation impact depends on the initial parameters of the uncorroded plate. One-millimetre thickness reduction in a plate with an initial thickness of 5 mm results in an insignificant change in the dispersion curve shape. In contrast, in the case of thinner plates, the difference is noticeable. There is no explicitly given relationship between the frequency, propagation velocity, and thickness reduction. However, for every thickness, frequencies of corrosion damage can be identified. The newly developed approach here aims to reconstruct the dispersion curve representing group velocity, enabling a better estimation of the average plate thickness during corrosion degradation.

The corrosion degradation level identification is based on measuring at least two signals by the transducers attached at two distinct positions. The distance between the actuator and sensors should be established by taking into account the dispersive nature of guided waves, signal attenuation, the energy of the input wave, and the size of the area, which is monitored. The shorter distance results in a greater signal-to-noise ratio (SNR), which facilities the interpretation of the results. The longer distance allows for assessing a greater area of the tested structure.

The algorithm presented here aimed at the reconstruction of dispersion curves using adjacent signals has been also analysed and utilized by other researchers (Draudviliene et al., 2021; Zima et al., 2022). The main development is its modification for group velocity extraction and employment in the corrosion degradation assessment. For clarity, a brief description of the following steps is presented here.

In the first step of the developed approach, the guided Lamb waves are excited by an actuator triggering a narrowband burst. In this study, the five-cycle sinusoid modulated by the Hann window is used (Lyons, 2011):

$$p(t) = \begin{cases} p_0 \sin\left(2\pi ft\right) \cdot w(t) & t \in \left[0, T_w\right] \\ 0 & t \geq T_w \end{cases}, \tag{2}$$

where f is the excitation frequency, p_0 denotes the excitation amplitude, and T_w is the modulating window length. The modulation window is described by a function:

$$w(t) = 0.5\left(1 - \cos\left(\frac{2\pi ft}{n_w}\right)\right), \quad t \in \left[0, T_w\right], \tag{3}$$

Next, the incident waves captured by sensors are identified and extracted from the adjacent signals (Figure 3, stage II). The reflections from the edges or other obstacles registered further in the signal are not considered, significantly simplifying the analysis, which is one of the most important advantages of this approach, especially in the context of the further research dedicated to diagnostics of large and complex structures. The trigonometric representations of the incident waves are calculated using the Fourier integral and the frequency response amplitude (Figure 3, stage III). The spectrum is normalised as the maximum value equals 1.0 in each case (Figure 3, stage IV). Based on the frequency ranges of the obtained spectra, the frequency limits f_L and f_H are established. In general, the spectrum vanishes above the upper-frequency limit f_H and below the lower frequency limit f_L (Figure 3, stage V). Regardless of the spectra' differences for signals registered during the same measurement, the frequency limits are the same. Next, the frequency spectra $S(f)$ are filtered by using n bandpass filters defined as a Gaussian magnitude function:

$$U_k(f) = S\left(f\right) B_k\left(f\right) = S(f) e^{4\ln(0.5)\left(\frac{f - f_L - (k-1)df}{\Delta B}\right)^2}, \tag{4}$$

and k=1, 2,…n. According to recommendations formulated by He (Ping He, 1998), the number of filters n depends on the bandwidth parameter ΔB, which defines the frequency range limited by the single filter:

$$n > 1 + \frac{f_H - f_L}{\Delta B}, \tag{5}$$

Here, the bandwidth parameter ΔB was determined based on the normalised Fourier frequency spectrum. Its value was established based on the spectrum width for the normalised amplitude corresponding to the -3dB value. In the next stage, the signal is synthesised from the basic trigonometric functions by using the inverse Fourier transform (Figure 3, stage VI).

Finally, the time of flight was determined by the envelope method. The envelope of the signal was calculated using the Hilbert transform (Figure 3, stage VII and VIII). The time of flight was computed using the cross-correlation method and was defined as the peak-to-peak value. The group velocity of Lamb waves was calculated as the distance x divided by the time of the flight. The shape of the dispersion curve was reconstructed by plotting the set of frequencies and corresponding group velocities (Figure 3, stage IX). Employing the group velocity instead of the phase velocity as a quality indicator significantly facilities the robustness of the developed procedure.

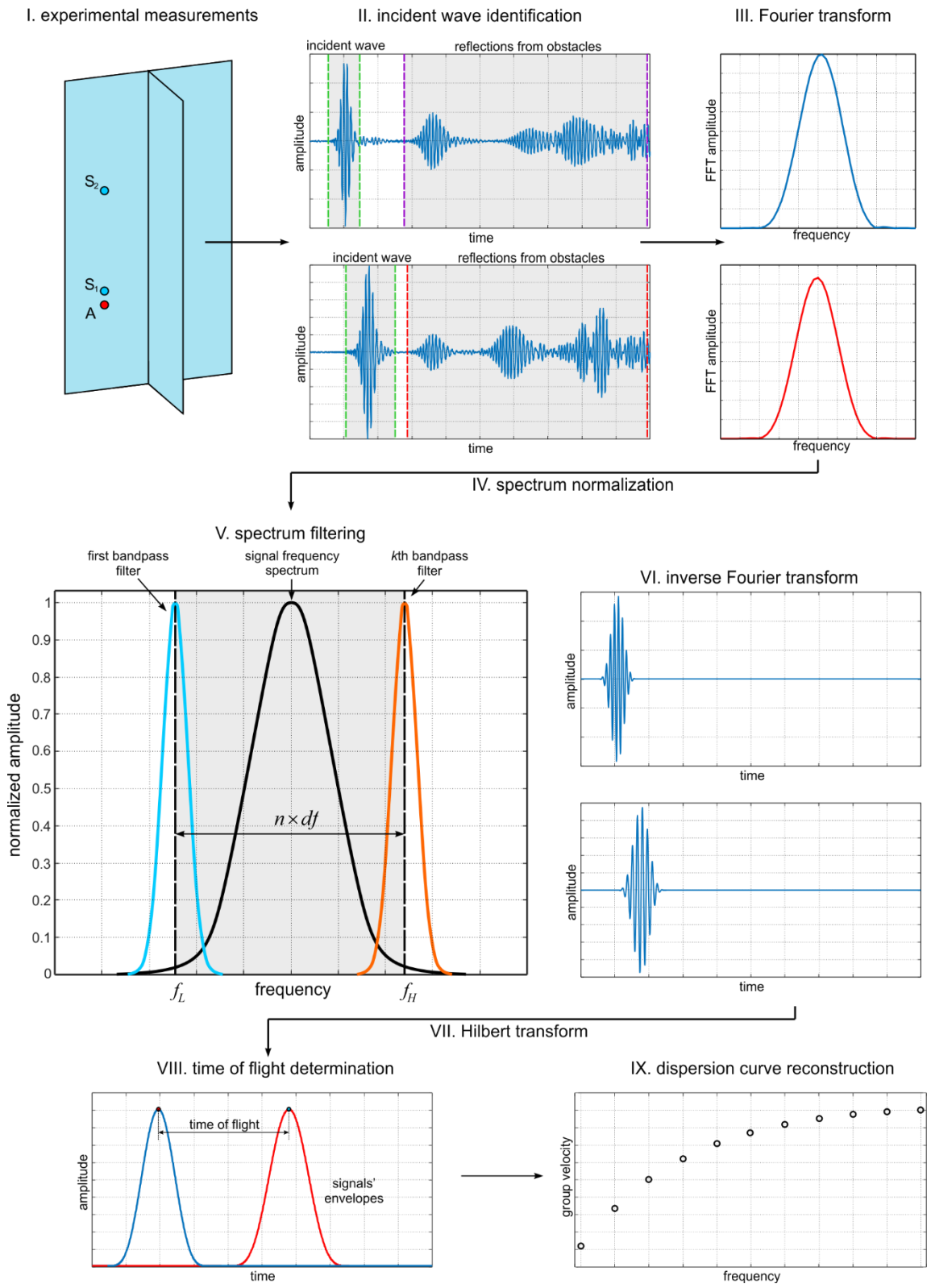

Figure 3 Signal processing procedure

The frequency range within the shape of the dispersion curve can be reconstructed based on the excitation frequency, the width of the signal spectrum, and spectra frequency limits f_L and f_H. In general, the segments of dispersion curves obtained for various frequencies may

overlap (Figure 4a). In such a case, the procedure has been extended by an additional step, and the group velocity was averaged within the common frequency region (Figure 4b).

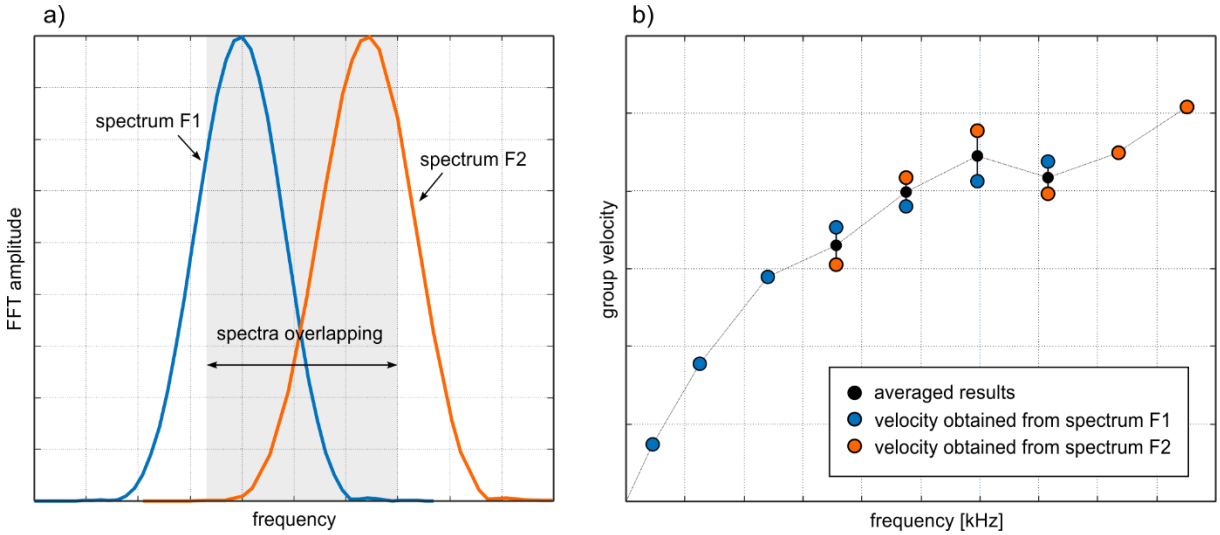

Figure 4 Processing of experimental data: a) spectra overlapping and b) averaging of group velocity determined in a common frequency range of both spectra

2.3 *Identification of corrosion degradation level*

To estimate the thickness reduction based on the reconstructed dispersion curve, first, the dependence for the first antisymmetric Lamb mode A_0 was calculated for the pre-established plate thickness *d*. Then, the dispersion curve determined numerically based on the analytical equation was considered as the sets of *n* pairs of numbers:

$$C_{gr}^{T}(d)=\left\{\left(\Delta f,c_{gr}^{T}(\Delta f)\right),\left(2\Delta f,c_{gr}^{T}(2\Delta f)\right),...,\left(n\Delta f,c_{gr}^{T}(n\Delta c_{gr})\right)\right\}=\left\{\left(\Delta f,c_{gr}^{T,1}\right),\left(2\Delta f,c_{gr}^{T,2}\right),...,\left(n\Delta f,c_{gr}^{T,n}\right)\right\}$$

The second set of data was obtained from the experimental analysis:

$$C_{gr}^{E}=\left\{\left(\Delta f,c_{gr}^{E}(\Delta f)\right),\left(2\Delta f,c_{gr}^{E}(2\Delta f)\right),...,\left(n\Delta f,c_{gr}^{E}(n\Delta c_{gr})\right)\right\}=\left\{\left(\Delta f,c_{gr}^{E,1}\right),\left(2\Delta f,c_{gr}^{E,2}\right),...,\left(n\Delta f,c_{gr}^{E,n}\right)\right\}$$

Next, the value of the following function has been calculated:

$$Y(d)=\frac{1}{n}\sum_{i=1}^{n}\left(y_i(d)\right)^2=\frac{1}{n}\sum_{i=1}^{n}\left(c_{gr}^{T,i}(d)-c_{gr}^{E,i}\right)^2 \tag{10}$$

The calculations were performed for a varying plate thickness. The function $Y(d)$ reached the minimum value for the best matching of numerical and experimental dispersion curves (Figure 5).

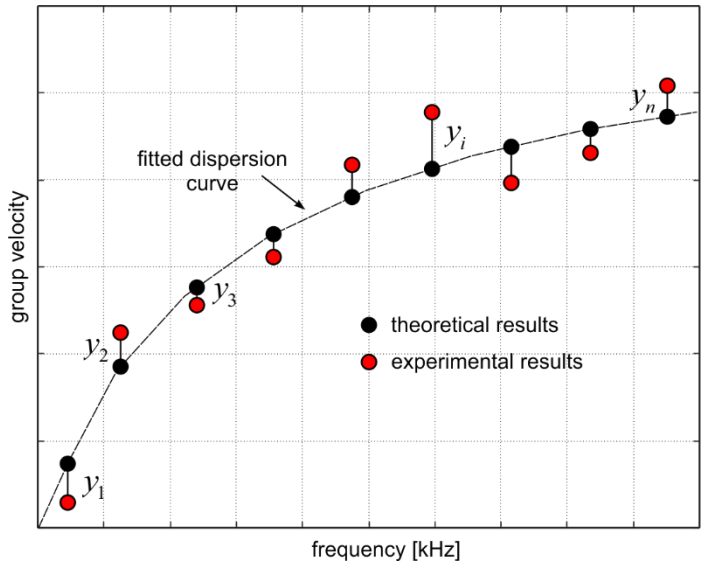

Figure 5 Matching of experimental and analytical results

In general, one can say that a similar effect in the form of a dispersion curve can be easily obtained using different excitation types i.e., broadband pulse excitation providing triggering multiple frequencies at the same time. This approach has been widely tested in corrosion assessment applications and its effectiveness in dispersion curve reconstruction based on Short Time Fourier Transform has been demonstrated. However, the broadband pulse excitation has several disadvantages which caused to decide to employ narrowband excitation. First of all, simultaneous excitation of several frequencies is associated with multiple wave mode excitation and further conversions. In the case of the specimens with more complex geometry and several modes varying in carrier frequency and velocity, it would be difficult to extract the part of the signal which should be processed. The second important reason is the possible application in real monitoring systems. Narrowband excitation associated usually with one single wave mode is much more effective in the detection of localized damage like corrosion pits or cracks. It is particularly important as long these two types of corrosion damage can occur simultaneously. Despite the fact this paper considers only general corrosion, the application of narrowband excitation potentially allows for both general corrosion degradation assessment (Zima et al., 2022), as well as the detection and localization of other damage types (Zima, 2021).

3 Experimental study

The experimental analysis of a stiffened steel plate was conducted, which is considered a primary structural component of the ship hull girder (Figure 6). The analysed stiffened plate was of 5 mm thickness, and its geometry is presented in Figure 6. The mechanical properties were determined via tensile tests of coupon specimens according to ISO standard (ISO, 2009).

The mean value from seven samples was estimated for the elastic modulus of 198 GPa and yield stress of 272.3 MPa.

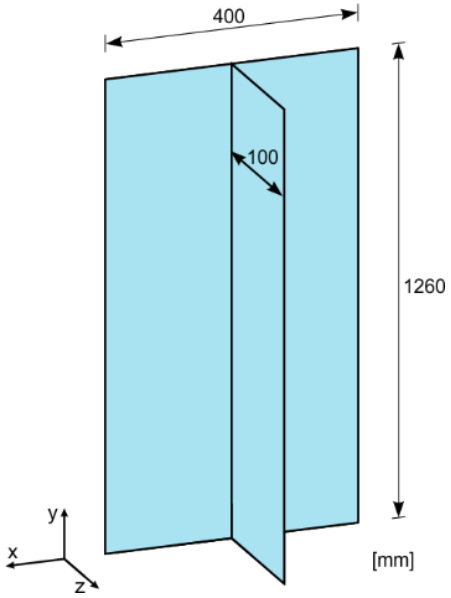

Figure 6. Stiffened plate geometry.

3.1 Corrosion degradation

The corrosion testing set-up was presented in (Woloszyk et al., 2021), together with the analysis of the generated corrosion degradation. The accelerated marine immersed corrosion degradation was generated by controlling the most important natural factors without applying DC. The specimens were placed in a 900-litre tank made from glass-reinforced plastic. The controlled environmental factors were the salinity (35 ppm), water circulation (induced by the circulation pumps), temperature (approx. 35 ℃, increased by heaters), and dissolved oxygen content (augmented by the aeration pump over the limit of fully saturated conditions). The periodical measurements of the stiffened plate specimen's mass were carried out using the scale with an accuracy of 2 g. Based on that, the propagation of each specimen's mean value corrosion diminution with the time was determined. The mean corrosion rate obtained for 5 mm specimens was equal to 0.774 mm/year, and the total duration of the corrosion tests was 428 days. In comparison to long-lasting experiments in natural seawater conditions, accelerated testing was a very efficient method. In real ship structures, the mean corrosion rate of the structures does not exceed the level of 0.1 mm/year (Melchers, 2008).

Three specimens of an initially 5 mm thickness were corroded, and three different degradation levels (calculated as the percentage loss of the initial mass of the specimen) were generated namely: 7%, 14% and 21%, by pulling the samples out of the water at different times. Although plate surfaces of different initial thicknesses were also corroded, the 5 mm plates

were chosen for validation of the new methodology. The thickness variability increased with the corrosion degradation level growth. Figure 7a shows the most severely corroded specimen, while Figure 7b presents the surfaces of any particular specimens.

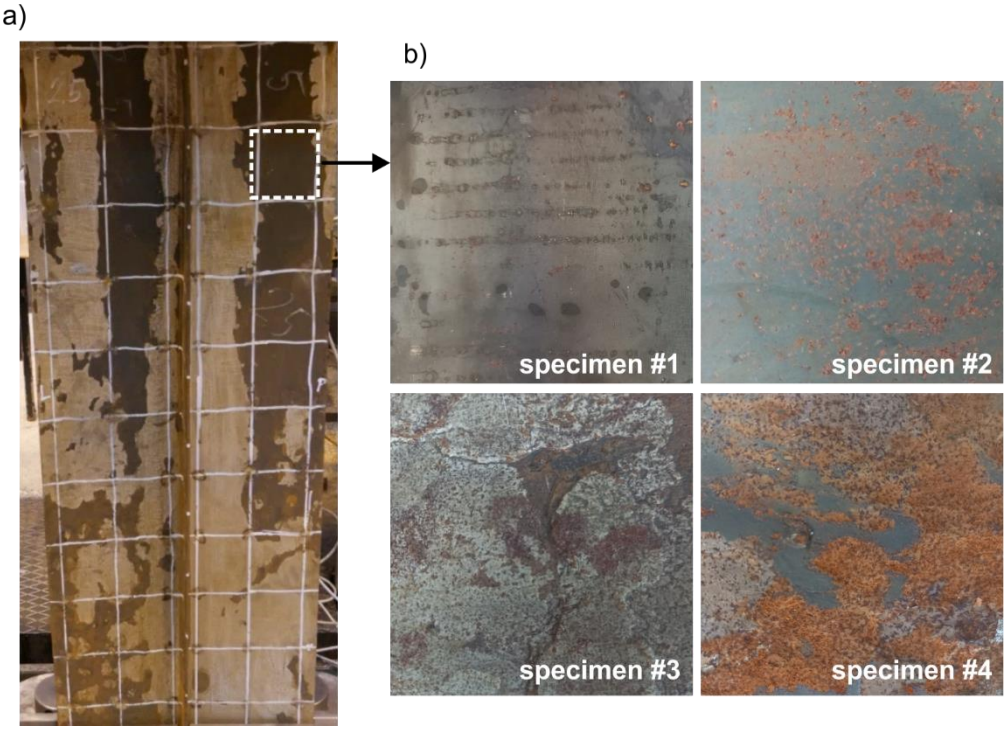

Figure 7 Corroded specimens: a) specimen with 21 % degradation level and b) surfaces of corroded specimens

It must be mentioned here that between environmental accelerated corrosion and the actual corrosion process some differences may occur, especially concerning the internal microstructure of the corroded element. However, the current study is mainly focused on the guided wave-based diagnostics method and recent studies (Zima, 2022) proved that the wave propagation velocity, as well as the time course of the signals, are dependent only on specimen thickness distribution. It means that two specimens varying in geometry but with the same thickness distribution will result in the same velocity and shape of the incident wave. Thus, the speed of the corrosion process has no direct influence on wave propagation signals but the resulting thickness variability and differences in specimen geometry may affect signal characteristics.

3.2 Guided wave propagation

The excitation and measurements of elastic waves were carried out by an experimental set-up comprised of an oscilloscope, function generator and piezoelectric transducers Noliac NAC2024. To improve the signal-to-noise ratio, the receiver was connected to the high voltage

amplifier ThorLab. The Lamb wave excitation was realised as a wave packet consisting of a five-cycle sine modulated by a Hann window. The carrier frequency was from 50 to 250 kHz with a step of 50 kHz (Figure 8a). The proposed algorithm has been tested for a low-frequency range to avoid the excitation of the higher-order modes. The sampling frequency was 500 MHz, and the input voltage was 20 V. To minimise the influence of electrical noises in the amplifier, each signal was averaged 1024 times. The perpendicular excitation is associated with triggering the propagation of flexural waves. Despite that, the presented reasoning is also valid for symmetric modes, from practical reasons it is much easier to attach the transducer at the plate surface rather than at the free edge. Therefore, further analysis concerns the antisymmetric Lamb modes defined by Eq. (1b).

The first signal was captured at 10 mm from the excitation source, while the second was 310 mm. The distance x between sensors was 300 mm (Figure 8c).

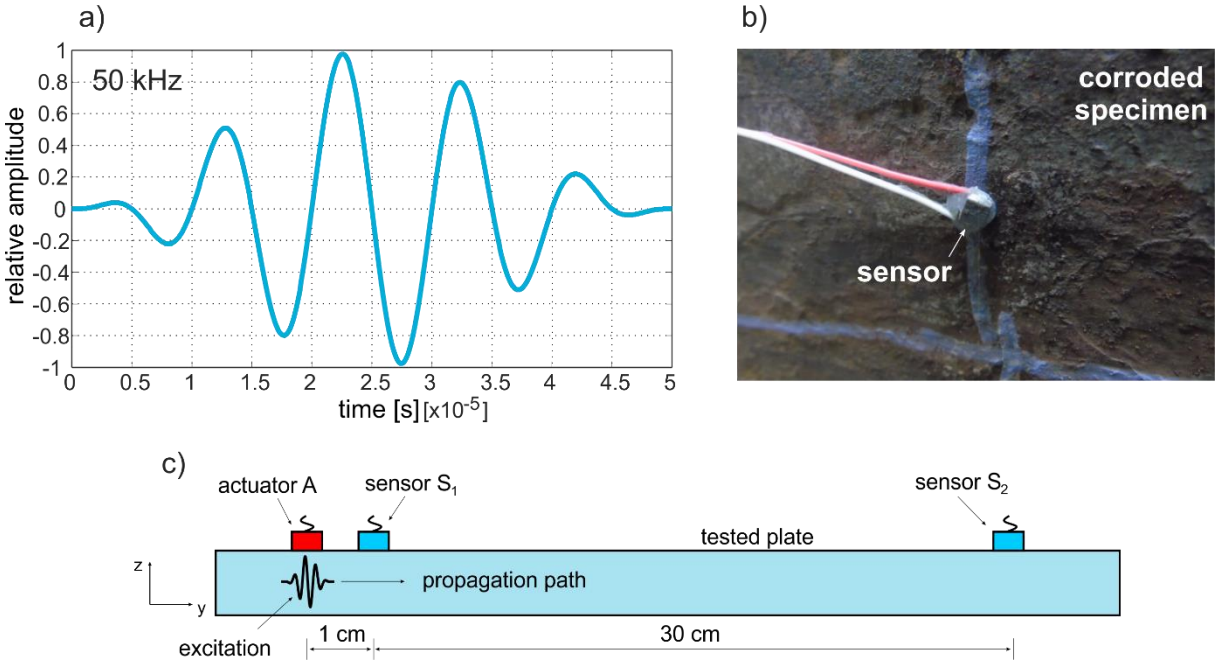

Figure 8 Experimental tests: a) excitation functions and b) sensor attached at the corroded plate surface, c) configuration of the transducers

The waves were propagated along the longer edge of the specimen (the propagation path was parallel to the stiffener). Such placement of the transducers allowed for avoiding the interference of reflections from edges and from stiffener with an incident wave which is further processed. Indeed, the influence of the additional structural elements should be included in further research. However, because the main aim of the present study is to develop and test the novel procedure of the corrosion degradation level assessment, we have used the favourable configuration of the transducers.

The reconstructed dispersion curve allows for assessing the corrosion degradation level along the propagation path. The longer the distance, the greater the monitored area, and the corrosion's thickness variability will be estimated as an equivalent average plate thickness.

The newly developed approach was tested in dispersion curve reconstruction on shorter distances not exceeding a few centimetres. The short distance minimises the dispersion effects and allows for a better characterisation of the corroded plate thickness variability as an equivalent average plate thickness. However, in large-scale offshore or ship structures, attaching sensors very close to each other would be inefficient. The distance of 30 cm was chosen to compromise the size of the monitored area of the stiffened plate and the resolution of the corrosion degradation plate surface roughness. Testing of more extended objects is possible with adequate amplifying of the excitation. It is also possible to use a different approach like multiple inputs-multiple outputs and a comprehensive sensor network to increase the monitored area.

4 Analysis and results

Wave propagation signals were processed to estimate the group propagation velocity for various frequencies and determine the average corroded plate thickness along the propagation path. The analysis was implemented in a MATLAB environment, and the adopted filtering parameters are summarised in Table 1.

Table 1 Parameters of the Gaussian filters

excitation frequency [kHz]	frequency limits [kHz]		filter bandwidth ΔB [kHz]	filters number K [-]
	f_L	f_H		
50	35	65	20	11
100	70	130	40	11
150	100	200	50	11
200	130	260	60	11
250	160	330	60	11

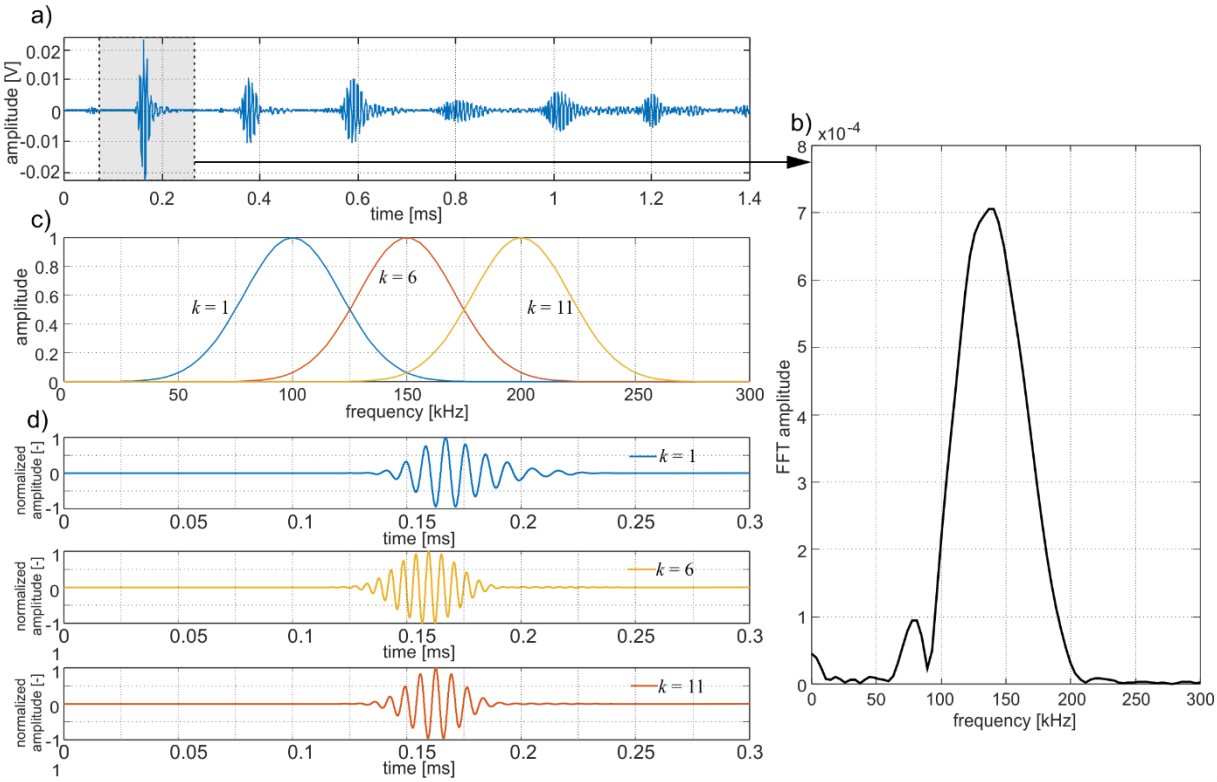

Figure 9 Signal processing: a) registered time-domain signal, b) Fourier transform of the extracted incident wave, c) filters and d) reconstructed signal after filtering

An exemplary signal captured by sensor S2 registering for the corroded plate (corrosion degradation level 7%) and the excitation frequency of 150 kHz, as well as the intermediate results in the form of a Fourier spectrum, filters, and three signals obtained for *k* equals to 1, 6 and 11 are presented in Figure 9.

The analysis has been divided into two stages. The dispersion curve has been reconstructed within the first stage based on the ten signals registered for five different frequencies. Thus, in total, ten signals were processed. In the second stage, the dispersion curve has been determined based on only two adjacent signals registered for one frequency.

4.1 Dispersion curve reconstruction based on several excitation frequencies

Figure 10 presents the results of reconstructing the dispersion curves for any particular specimens. Experimental outcomes are denoted by red dots, while the solid black line depicts the Lamb dispersion curve characterised by the minimal value of $Y(d)$ (Eqn 10). Despite the experimental group velocity coinciding well with the dispersion curve, the difference in matching the analytical solution is visible, confirming the correctness of the proposed algorithm of dispersion curve reconstruction. The most significant deviation of experimental results from the theoretical curve was obtained for the specimen characterised by the highest corrosion degradation level (Figure 10d), which the more intense wave integration may cause with

irregularities of the corroded surface, as well as with the most significant deviation of the plate thickness from the average value.

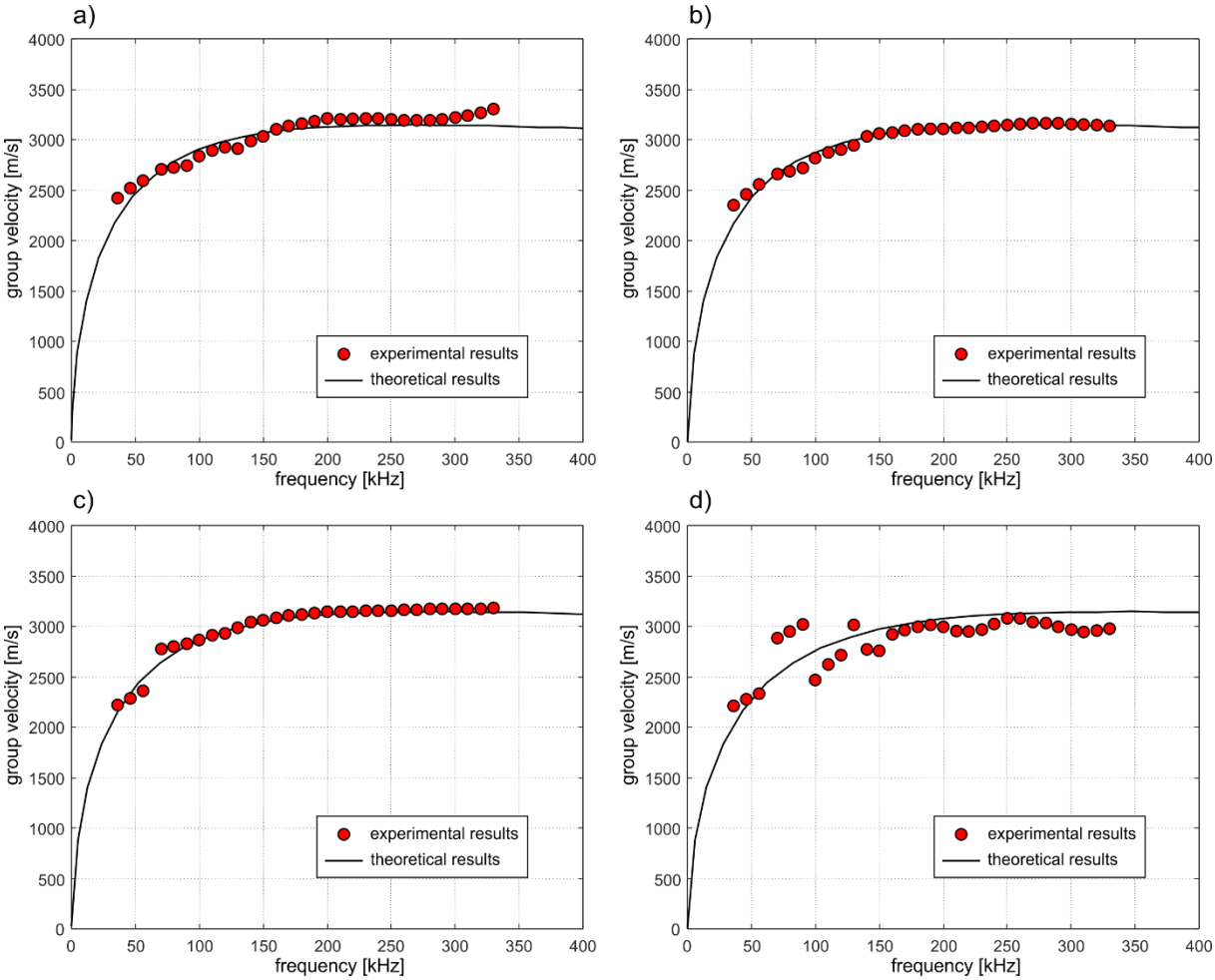

Figure 10 Reconstruction of dispersion curves for a) specimen #1, b) specimen #2, c) specimen #3 and d) specimen #4

The estimated parameters of the analysed corroded plates are summarised in Table 2. The estimated corrosion level C_a has been calculated based on the determined plate thickness from the fitted dispersion curve:

$$C_d = \frac{d_t}{d} \cdot 100\%, \tag{11}$$

where d is the thickness of the uncorroded plate determined non-destructively, and d_t is the thickness of the corroded plate, where d was estimated as 5.18 mm. Comparing the results for corroded and uncorroded plates, it can be seen that the guided wave propagation approach limits the inaccuracies of determination of propagation velocity caused by the chosen method of the time-of-flight calculation and the influence of deviation of material parameters. On the other hand, the reference signals registered for the original structure are required for such comparison. Still, it can be noticed that the reference measurement does not have to be made on the same structure.

The estimated corrosion degradation levels differ slightly from the actual one, but a good agreement between the results is observed. The absolute error, which is defined as the difference between the accurate and estimated equivalent average thickness:

$$e_a = \left| d_a - d_t \right| \tag{13}$$

did not exceed 0.5 mm, which indicates that the plate thickness may be estimated with high accuracy even without reference measurements. The maximum value of the relative error referencing to actual thickness:

$$e_r = \frac{e_a}{d_a} \cdot 100\%, \tag{14}$$

is equal to 10.42% and was obtained for specimen #3 but is can be explained by the fact that the general corrosion is not associated with perfect uniform thickness reduction. The higher corrosion level C_d does not exclude that in some regions the thickness reduction is smaller and opposite.

Table 2 Average corrosion degradation level of stiffened plates

specimen	actual corrosion level C_d [%]	average thickness d_a [mm]	thickness determined by Lamb waves d_t [mm]	estimated corrosion level C_a [%]	absolute error e_a [mm]	relative error e_r [%]
#1	0	5	5.180	0	0.180	2.40
#2	7	4.638	4.890	4.500	0.252	5.43
#3	14	4.320	4.770	6.835	0.450	10.42
#4	21	3.948	4.000	21.875	0.052	1.32

4.2 Dispersion curve reconstruction based on one excitation frequency

An attempt of corrosion degradation assessment based on one excitation frequency and only one pair of signals captured at points S1 and S2 were made. The segment of the dispersion curve has been reconstructed based on the measurement made for an excitation frequency of 150 kHz. Based on the theoretical solution traced for uncorroded plate (Figure 2), one can conclude that relatively low frequencies (<100 kHz) are highly dispersive, which means that low-frequency change results in a significant alteration in the propagation velocity. Consequently, the shape of the propagating wave packet varies significantly along the propagation path. The potential inaccuracies in measuring the distance between sensors or calculating the flight time result in a substantial over-or underestimation of the propagation velocity. Despite that this frequency range seems to be sensitive to plate thickness changes, the reconstruction of the dispersion curve may be laden with a substantial error.

In turn, for the high frequencies (>200 kHz), the dispersion curve becomes flat, the velocity for various frequencies is similar, and the shape of the propagating wave packet remains unchanged. Moreover, the higher the frequency, the shorter the wave becomes and thus is much more sensitive to the surface irregularities caused by corrosion degradation. In the signal, additional reflections are registered, which hinders the unambiguous indication and further extraction of incident waves for the analysis. The wave energy is dissipated faster, and the SNR decreases. Moreover, one can see that the higher frequencies become insensitive to the thickness reduction. The plate thickness reduction is associated with an insignificant propagation velocity change. Considering all aspects mentioned above, a "medium" frequency of 150 kHz is used, which is a compromise between dispersion effects, SNR, and sensitivity to corrosion damage.

Figure 11 depicts the experimental group velocities and reconstructed dispersion curves, while the corrosion degradation level assessment is summarised in Table 3. The corrosion degradation level assessment accuracy is lower when the curve is traced based on only one measurement. However, still, a good agreement between actual and estimated corrosion degradation levels was noted. In all cases, the corrosion degradation level has been overestimated. However, the absolute error did not exceed 0.8 mm.

The most significant deviations of experimental outcomes from the theoretical solution are observed at the ends of the considered frequency range for the highest and the lowest frequency components of the fundamental antisymmetric mode (100 and 200 kHz). The main reason may be the presence of the side lobes, which were not eliminated from the frequency spectrum despite windowing the input signal and subsequent filtering the Fourier spectrum (Lyons, 2011). The same effect was also observed in the previous investigation stage for other frequencies. Still, the averaging of overlapping curve segments at the ends of the frequency range (Figure 4b) reduced the deviations from the theoretical curve.

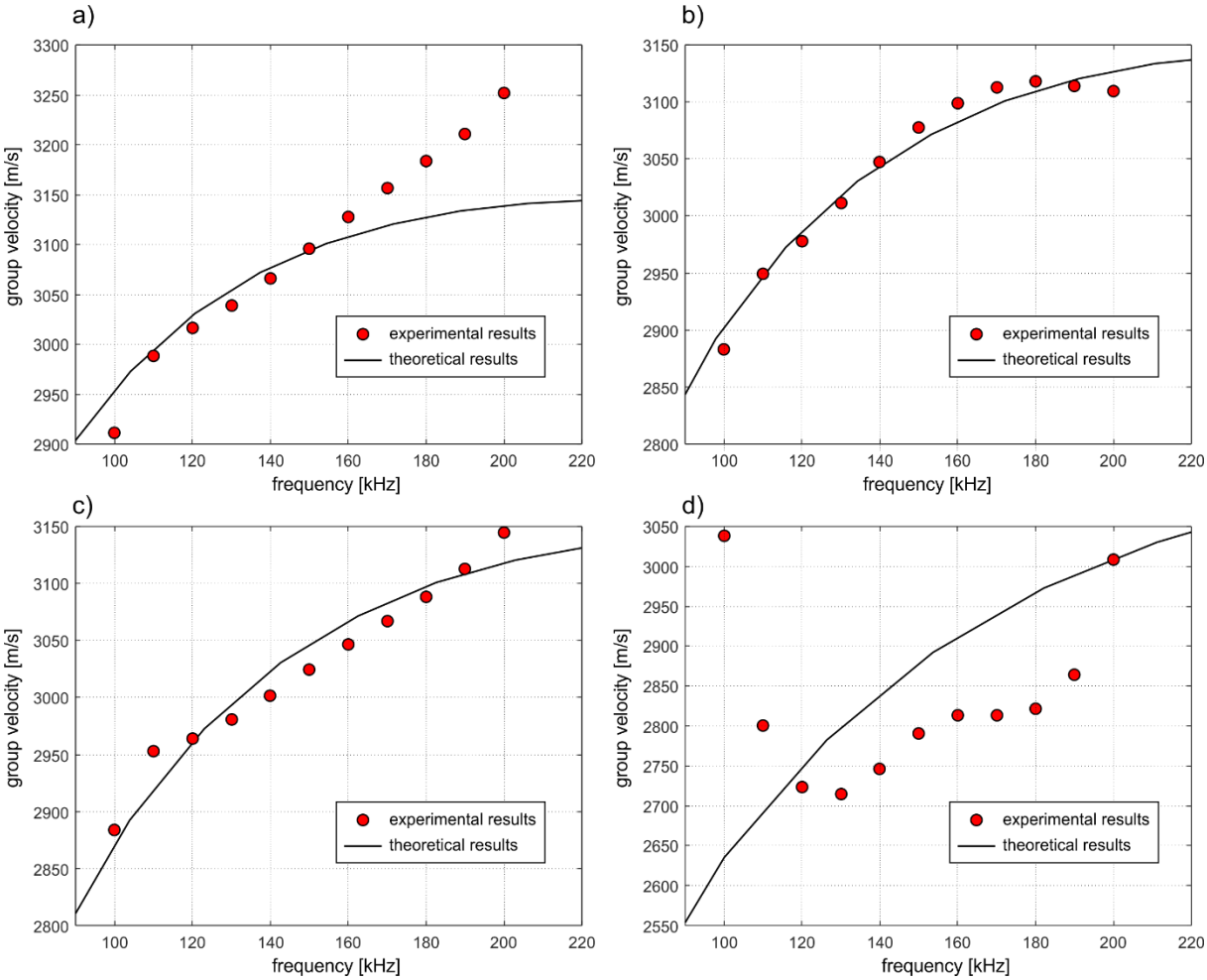

Figure 11 Reconstruction of dispersion curves for a) specimen #1, b) specimen #2, c) specimen #3 and d) specimen #4

Table 3 Corrosion degradation level of stiffened plates

specimen	actual corrosion level C_d [%]	average thickness d_a [mm]	thickness determined by Lamb waves d_t [mm]	estimated corrosion level C_a [%]	absolute error e_a [mm]	relative error e_r [%]
#1	0	5	5.770	0	0.770	15.40
#2	7	4.638	5.170	10.399	0.532	11.47
#3	14	4.320	4.870	15.598	0.550	12.73
#4	21	3.948	3.290	42.981	0.658	16.67

4.3 Calibration and error mitigation

There are several different sources of inaccuracies where one of the most compelling reasons in the applied approach is the time of the flight. In this study, the time of flight was defined as a difference in the registration time of the peaks of the signal envelopes determined by using the cross-correlation method. However, there are many developed approaches for flight estimation, and the results differ slightly depending on which method was chosen (Xu et al., 2009). Because the thickness was overestimated in most cases, one can conclude a

systematic error made during the velocity determination. In the considered frequency range, the increase of velocity is related to an increase in the thickness. Thus, possibly the applied method of the time of flight determination based on cross-correlation of the Hilbert transform of adjacent signals resulted in underestimating the registration time.

To investigate whether the systematic error of velocity determination influenced the results, the following analysis has been conducted: based on the analytical and experimental dispersion curves obtained for an undamaged plate with a known thickness of d = 5 mm., the error has been determined. The velocity overestimation was Δ =19 m/s. The velocities obtained for other stiffened plates have been reduced by Δ, which means that the obtained curves were just shifted down without changing their shapes, and then the procedure of the corrosion level identification has been applied (Section 2.3). Table 4 contains the results obtained after calibrating the velocity based on an uncorroded plate. It is visible that calibrating the velocity increases the quality of the estimated corrosion degradation level. It is noted, that in most cases, the presented method overestimates the thickness. However, for Specimen #4, the thickness is underestimated. At that stage of development, this does not allow to make some general conclusions regarding that issue and future studies are needed. The error influence may be limited by conducting the measurements for various frequencies and various distances between the transducers.

Table 4 Corrosion degradation level of stiffened plates after velocity calibration

specimen	actual corrosion level [%]	corrosion level estimated based on Lamb waves [%]	
		without velocity calibration	with velocity calibration
#1	0	0	0
#2	7	10.399	5.200
#3	14	15.598	9.500
#4	21	42.981	20.00

4.4 Discussion

The results presented in the previous section confirm the proposed algorithm's effectiveness in tracing the dispersion curve and identifying the averaged structural degradation level. The main advantage over so far presented ultrasonic methods dedicated to thickness estimation of corroded ship's structural components is the necessity to collect a limited number of signals. The transducers network does not demand a large number of PZT. The actuator triggered the signals was captured by two sensors and one actuator placed on a line. The first sensor should be attached at a short distance from an actuator, which provides a high-amplitude

incident wave. The spatial distance between the sensors can be adjusted to the structure size, used equipment, and the desired accuracy of identifying the average corroded plate thickness.

A significant advantage is that the presented wave-based method does not require collecting the reference data for an uncorroded structure. The measurements of uncorroded plates improve the quality of the results obtained and allow for better corrosion degradation assessment by reducing the influence of systematic errors, but they are not indispensable.

The robustness of the novel procedure was examined in two stages. In the first stage, the group velocity dispersion curve has been reconstructed using signals registered for various excitation frequencies. The main advantage of the approach based on the measurement of several frequencies is that the shape of the dispersion curve can be faithfully reconstructed. On the other hand, the number of required signals and, in consequence, the time of analysis is longer. In the second stage, the signals were registered for only one excitation type. The main advantage of reconstructing only one chosen segment of the dispersion curve is the necessity to use only one excitation frequency for all tested specimens. The assessment of the corrosion degradation demands only two signals be captured at the known distance. However, it also demands the appropriate choice of excitation frequency, which is not a trivial issue and requires considering the shape of the dispersion curve determined based on an analytical equation.

Despite promising results, the indispensable prerequisite of the further enhancement of the proposed approach demanded before its practical application is the consideration of its limitations. First, the corrosion degradation identification algorithm does not take into account the plate thickness variability. The corrosion degradation level was indirectly averaged by assuming that the thickness is constant along the propagation path. However, the plate thickness variability can be mapped much better by extending the sensors network or taking additional measurements at other points.

The irregularities of the corroded surfaces influenced the quality of the results. The disturbance interactions with abnormalities resulting in wave diffractions and conversions lead to incident wave indication and extraction difficulties for further analysis. Though only one antisymmetric wave mode could propagate within the considered frequency range, wave integration with irregular surfaces might also induce low-energy symmetric wave mode. Propagating of multiple wave packets and their interference affects the shape of the incident wave and, in consequence, the characteristics of the frequency spectrum, which led to inaccuracies in time of flight estimation.

The discrepancies between theoretical and experimental results can also originate from the assumption about the constant value of elastic modulus and material density; however, the

material parameters are also predefined in standard ultrasonic thickness measurement to calculate the velocity of the pressure wave. Thus, further development of the corrosion degradation level identification algorithm may include the impact on material parameters or fluctuations on the dispersion curve shape. The dependence between wave velocity and any parameter in the dispersion Lamb equation is strongly nonlinear, which means that, e.g., the overestimation of elastic modulus may lead to overestimating wave velocity for one excitation frequency and underestimating for other frequencies. It should be noted that the influence of corrosion degradation on material properties was not considered here. The density, Poisson's ratio, and elastic modulus were assumed the same for all analysed stiffened plates.

The next element necessary to consider in further studies is the influence of the additional structural elements affecting wave propagation. The problem of the additional reflections can be solved in two different ways. In general, guided wave-based algorithms are usually used for processing the data collected by specially designed SHM systems. In such cases, signals are measured for various states of the investigated specimen and the reference measurements are available for the investigators. Particular reflections can be identified and interpreted and next excluded on the further stages of monitoring and signal processing. The second way to limit the problem of additional reflections from boundaries and stiffeners is the utilization of different transducer types. Recently, a novel type of frequency steerable transducers has been developed. The novel transducer allows sending of the signal only in one chosen direction, which is dependent on the excitation frequency (Baravelli et al., 2013; De Marchi et al., 2016). The main lobe, characterized by high amplitude propagates in one direction while small-amplitude side lobes propagate in other directions. Even if the total elimination of the boundaries reflections is not possible, their amplitudes can be significantly reduced by focusing wave energy only in an interesting direction.

5 Future perspectives

Since the present study mainly focused on the development of the signal processing which can be potentially used in the SHM systems, several aspects were not considered here and should be investigated in future studies, including:

- Ships and offshore structures are large in size and complex in geometry. Their diagnostics would require a more complex sensor network. The optimal sensor placement will be considered. The trade-off between the resolution and extent of the sensors network must be considered.
- Practical application of the developed approach requires considering the reliability of the proposed method and the influence of inaccuracies on the determined DoD (Falcetelli et

al., 2021). This should in particular cover further studies regarding higher thicknesses of analysed plates and related uncertainty levels.

- Guided waves are widely used for localized damage detection. Therefore, the possibility of building multi-step algorithms for both general uniform and pitting corrosion detection and evaluation must be investigated.

6 Conclusions

This study conducted theoretical and experimental investigations of guided wave propagation in corroded stiffened plates. The newly developed approach allows for an average corrosion degradation level identification based on the single measurements of the tested stiffened plates.

The experimental data acquired for four different stiffened plates varying in degradation level confirmed the correctness of the developed procedure of dispersion curve reconstruction. The corrosion degradation level identification has been made in several different ways: once the dispersion curve has been traced based on several measurements made for various frequencies. At the same time, in the second case, the signals were captured for only one excitation type. It was proved that the corrosion degradation level was better assessed if the measurements involved a wider frequency range. However, regardless of the considered frequency range within the dispersion curve that has been reconstructed, the corrosion degradation level remained slightly underestimated, which indicated the possible systematic error related to the time of flight and, in consequence, with group velocity estimation. Based on the assumption that the initial thickness of the uncorroded stiffened plate is usually known a priori, the value of systematic error has been established and included in further assessing the corrosion deterioration of other stiffened plates. It allowed for a better estimation of the precise degree of corrosion degradation.

The highest deviation between experimental measurements and theoretically defined dispersion curve was observed for the most severely corroded stiffened plates. This allows the hypothesis that the presented methodology could determine the average thickness and its variability level. After further development, the proposed method should be applicable in all cases requiring multiple ultrasonic measurements to assess the thickness of steel structural elements.

Acknowledgement

The first author greatly acknowledges the support of the Foundation for Polish Science (FNP).

References

Baravelli E, Senesi M, Ruzzene M, De Marchi L. Fabrication and Characterization of a Wavenumber-Spiral Frequency-Steerable Acoustic Transducer for Source Localization in Plate Structures. IEEE Trans Instrum Meas 2013;62:2197–204. https://doi.org/10.1109/TIM.2013.2255992.

Cao X, Zeng L, Lin J. Generalized scattering matrix method for Lamb wave scattering analysis at cascaded notches. J Vib Control 2021:107754632110377. https://doi.org/10.1177/10775463211037790.

Cegla F, Gajdacsi A. Mitigating the effects of surface morphology changes during ultrasonic wall thickness monitoring. AIP Conf. Proc., 2016, p. 170001. https://doi.org/10.1063/1.4940624.

Ciampa F, Scarselli G, Pickering S, Meo M. Nonlinear elastic wave tomography for the imaging of corrosion damage. Ultrasonics 2015;62:147–55. https://doi.org/10.1016/j.ultras.2015.05.011.

Ding X, Xu C, Deng M, Zhao Y, Bi X, Hu N. Experimental investigation of the surface corrosion damage in plates based on nonlinear Lamb wave methods. NDT E Int 2021;121:102466. https://doi.org/10.1016/j.ndteint.2021.102466.

Draudviliene L, Tumsys O, Mazeika L, Zukauskas E. Estimation of the Lamb wave phase velocity dispersion curves using only two adjacent signals. Compos Struct 2021;258:113174. https://doi.org/10.1016/j.compstruct.2020.113174.

Ervin BL, Kuchma DA, Bernhard JT, Reis H. Monitoring Corrosion of Rebar Embedded in Mortar Using High-Frequency Guided Ultrasonic Waves. J Eng Mech 2009;135:9–19. https://doi.org/10.1061/(ASCE)0733-9399(2009)135:1(9).

Ervin BL, Reis H. Longitudinal guided waves for monitoring corrosion in reinforced mortar. Meas Sci Technol 2008;19:055702. https://doi.org/10.1088/0957-0233/19/5/055702.

Falcetelli F, Yue N, Di Sante R, Zarouchas D. Probability of detection, localization, and sizing: The evolution of reliability metrics in Structural Health Monitoring. Struct Heal Monit 2021:147592172110607. https://doi.org/10.1177/14759217211060780.

Farhidzadeh A, Salamone S. Reference-free corrosion damage diagnosis in steel strands using guided ultrasonic waves. Ultrasonics 2015;57:198–208. https://doi.org/10.1016/j.ultras.2014.11.011.

Flashback history: Tanker Prestige sinking (Video). 2015.

Howard R, Cegla F. Detectability of corrosion damage with circumferential guided waves in reflection and transmission. NDT E Int 2017;91:108–19. https://doi.org/10.1016/j.ndteint.2017.07.004.

Hu M, He J, Zhou C, Shu Z, Yang W. Surface damage detection of steel plate with different depths based on Lamb wave. Measurement 2022;187:110364. https://doi.org/10.1016/j.measurement.2021.110364.

Hua J, Cao X, Yi Y, Lin J. Time-frequency damage index of Broadband Lamb wave for corrosion inspection. J Sound Vib 2020;464:114985. https://doi.org/10.1016/j.jsv.2019.114985.

ISO. Metallic materials - Tensile testing - Part 1: Method of test at room temperature. Int Stand ISO 6892-1 2009.

Lamb H. On waves in an elastic plate. Proc R Soc London Ser A, Contain Pap a Math Phys Character 1917;93:114–28. https://doi.org/10.1098/rspa.1917.0008.

Li Z, Wang Y, Zheng J, Liu N, Li M, Teng J. Stress measurement for steel slender waveguides based on the nonlinear relation between guided wave group velocity and stress. Measurement 2021;179:109465. https://doi.org/10.1016/j.measurement.2021.109465.

Lyons R. Understanding Digital Signal Processing. 3rd ed. Prentice-Hall; 2011.

De Marchi L, Testoni N, Marzani A. A New Generation of Frequency Steerable Transducers for Lamb Waves Inspections. 19th World Conf. Non-Destructive Test. (WCNDT 2016), Munich: 2016, p. 1–8.

Melchers RE. Development of new applied models for steel corrosion in marine applications including shipping. Ships Offshore Struct 2008;3:135–44. https://doi.org/10.1080/17445300701799851.

Moustafa A, Niri ED, Farhidzadeh A, Salamone S. Corrosion monitoring of post-tensioned concrete structures using fractal analysis of guided ultrasonic waves. Struct Control Heal Monit 2014;21:438–48. https://doi.org/10.1002/stc.1586.

Panayotova M, Garbatov Y. Corrosion of steels in marine environment, monitoring and standards. Saf. Reliab. Ind. Prod. Syst. Struct., CRC Press; 2010, p. 369–413. https://doi.org/10.1201/b10572-36.

Parunov J, Senjanović I, Guedes Soares C. Hull-girder reliability of new generation oil tankers. Mar Struct 2007;20:49–70. https://doi.org/10.1016/j.marstruc.2007.03.002.

Ping He. Simulation of ultrasound pulse propagation in lossy media obeying a frequency power law. IEEE Trans Ultrason Ferroelectr Freq Control 1998;45:114–25. https://doi.org/10.1109/58.646916.

Sharma S, Mukherjee A. Longitudinal Guided Waves for Monitoring Chloride Corrosion in Reinforcing Bars in Concrete. Struct Heal Monit 2010;9:555–67. https://doi.org/10.1177/1475921710365415.

Tian Z, Xiao W, Ma Z, Yu L. Dispersion curve regression – assisted wideband local wavenumber analysis for characterizing three-dimensional (3D) profile of hidden corrosion damage. Mech Syst Signal Process 2021;150:107347. https://doi.org/10.1016/j.ymssp.2020.107347.

Wandowski T, Malinowski P, Ostachowicz WM. Damage detection with concentrated configurations of piezoelectric transducers. Smart Mater Struct 2011;20:025002. https://doi.org/10.1088/0964-1726/20/2/025002.

Woloszyk K, Garbatov Y, Kowalski J. Indoor accelerated controlled corrosion degradation test of small- and large-scale specimens. Ocean Eng 2021;241:110039. https://doi.org/10.1016/j.oceaneng.2021.110039.

Woloszyk K, Kahsin M, Garbatov Y. Numerical assessment of ultimate strength of severe corroded stiffened plates. Eng Struct 2018;168:346–54. https://doi.org/10.1016/j.engstruct.2018.04.085.

Xiao L, Peng J, Zhang J, Ma Y, Cai CS. Comparative assessment of mechanical properties of HPS between electrochemical corrosion and spray corrosion. Constr Build Mater 2020;237:117735. https://doi.org/10.1016/j.conbuildmat.2019.117735.

Xu B, Yu L, Giurgiutiu V. Advanced methods for time-of-flight estimation with application to Lamb wave structural health monitoring. Proc. 7th Int. Work. Struct. Heal. Monit., Palo Alto, CA, USA: 2009.

Yuan Y, Ji Y, Shah S. Comparison of Two Accelerated Corrosion Techniques for Concrete Structures. ACI Struct J 2007;104:344–7. https://doi.org/10.14359/18624.

Zayed A, Garbatov Y, Guedes Soares C. Corrosion degradation of ship hull steel plates accounting for local

environmental conditions. Ocean Eng 2018;163:299–306. https://doi.org/10.1016/j.oceaneng.2018.05.047.

Zayed A, Garbatov Y, Guedes Soares C. Non-destructive Corrosion Inspection Modeling of Tanker Structures. Vol. 2 Struct. Saf. Reliab., ASMEDC; 2008, p. 465–76. https://doi.org/10.1115/OMAE2008-57500.

Zima B. Determination of stepped plate thickness distribution using guided waves and compressed sensing approach. Measurement 2022;196:111221. https://doi.org/10.1016/j.measurement.2022.111221.

Zima B. Damage detection in plates based on Lamb wavefront shape reconstruction. Measurement 2021;177:109206. https://doi.org/10.1016/j.measurement.2021.109206.

Zima B, Rucka M. Guided wave propagation for assessment of adhesive bonding between steel and concrete. Procedia Eng 2017;199:2300–5. https://doi.org/10.1016/j.proeng.2017.09.189.

Zima B, Woloszyk K, Garbatov Y. Corrosion degradation monitoring of ship stiffened plates using guided wave phase velocity and constrained convex optimization method. Ocean Eng 2022;253.